HHS Public Access

Author manuscript

Neuroimage. Author manuscript; available in PMC 2021 July 15.

Published in final edited form as:

Neuroimage. 2020 July 15; 215: 116853. doi:10.1016/j.neuroimage.2020.116853.

Neuroimaging contrast across the cortical hierarchy is the feature maximally linked to behavior and demographics

Feng Han[a], **Yameng Gu**[a], **Gregory L. Brown**[b], **Xiang Zhang**[c], **Xiao Liu**[a,d,*]

[a]Department of Biomedical Engineering, The Pennsylvania State University, PA, USA

[b]Department of Engineering Science and Mechanics, The Pennsylvania State University, PA, USA

[c]College of Information Sciences and Technology, The Pennsylvania State University, PA, USA

[d]Institute for Computational and Data Sciences, The Pennsylvania State University, PA, USA

Abstract

An essential task of neuroscience is to elucidate the relationship between brain activity, brain structure, and human behavior. This study aims to understand this 3-way relationship by studying the population covariance of resting-state functional connectivity, cortical thickness, and behavioral/demographic measures in a large cohort of individuals. Using a data-driven canonical correlation analysis, we found that maximal pairwise correlations between the three modalities are approximately along the same direction across subjects, which is characterized by the change of the overall positive-negative trait of human behavior. More importantly, this behavioral change is associated with a divergent modulation of both resting-state connectivity and cortical thickness across cortical hierarchies between the higher-order cognitive networks and lower-order sensory/motor regions. The findings suggest that the cross-hierarchy contrast of structural and functional brain measures is tightly linked to the overall positive-negative trait of human behavior/demographics.

Keywords

Brain hierarchy; Cortical thickness; Resting-state fMRI connectivity; Behavioral and demographic measures; Canonical correlation analysis

*Corresponding author. 431 Chemical and Biomedical Engineering Building (CBEB), The Pennsylvania State University, University Park, PA, 16802-4400, USA. xxl213@engr.psu.edu (X. Liu).

Author contributions

Feng Han: Conceptualization, Methodology, Software, Formal Analysis, Investigation, Writing - Original Draft, Validation and Visualization. **Xiao Liu**: Supervision, Methodology, Software, Writing - Review & Editing, Visualization, Funding Acquisition and Project Administration. **Yameng Gu**: Resources, Writing - Review & Editing, Visualization. **Gregory L. Brown**: Resources, Writing - Review & Editing. **Xiang Zhang**: Supervision, Resources, Writing - Review & Editing.

Declaration of competing interest

None.

Appendix A. Supplementary data

Supplementary data to this article can be found online at https://doi.org/10.1016/j.neuroimage.2020.116853.

1. Introduction

Understanding the neural and structural basis of behavioral variability across individuals is an important task for neuroscience. Modern neuroimaging research has made significant progress towards this goal through the study of the brain-behavior relationship across individuals (Bullmore and Sporns, 2009; Goldstein and Volkow, 2011; Kanai and Rees, 2011). The advent of resting-state functional magnetic resonance imaging (fMRI) enabled a non-invasive measurement of functional brain connectivity (Biswal et al., 1995), which has been linked to a variety of individual measures, such as demographic factors (Dohmen et al., 2011), lifestyle (Topiwala et al., 2018), and cognitive functions (Miller et al., 2016; Rosenberg et al., 2015). A comprehensive study of this connectivity-behavior relationship was recently made possible by the Human Connectome Project (HCP), which collected resting-state fMRI data along with hundreds of behavioral, cognitive, psychometric, and demographic measures from a large cohort of 1,200 subjects (Van Essen et al., 2013). A data-driven canonical correlation analysis (CCA) (Hotelling, 1936) to the HCP data revealed only a single significant CCA mode of population covariation that maximally links individuals' functional connectivity with their demographic/behavioral measures. Interestingly, a characteristic pattern of behavioral changes emerges in this mode direction with individuals showing more positive subject traits, such as good performance on memory and cognitive tests, high life satisfaction, and good education, towards one end but more negative ones, such as substance use, rule-breaking behavior, and anger, towards the other (Smith et al., 2015).

However, structural and morphological brain changes along this specific "positive-negative" mode maximally linking the functional connectivity and behavioral/demographic measures remain unclear, even though both modalities have been linked to structural/morphometric brain properties separately. For example, the resting-state connectivity has been linked to structural connectivity measured with diffusion imaging (Honey et al., 2009), microstructural properties such as cortical myelination (Huntenburg et al., 2017), and morphometric measures such as the cortical thickness (Deepak Pandya, Benjamin Seltzer, Michael Petrides, 2015). On the other hand, inter-subject variability in brain structures and morphology, particularly the cortical thickness, has been repeatedly linked to individual differences in various subject measures, including intelligence, aggression, and life satisfaction (Choi et al., 2008; Kanai and Rees, 2011; Karama et al., 2011; Ly et al., 2012; Narayan et al., 2007; Narr et al., 2007; Thijssen et al., 2015; Zhu et al., 2018). Notably, a recent comprehensive study on the relationship between various structural imaging properties and behavioral/demographic measures has identified a direction also featured by the positive-negative change of behaviors (Llera et al., 2019). However, it remains elusive how this structure-behavior mode is correspondent to the connectivity-behavior mode. Therefore, it would be interesting to know whether this positive-negative mode of connectivity-behavior covariation is associated with changes in certain structural/morphometric brain properties. If so, would this association also represent the maximal correlation between this structural/morphometric property and the other two modalities? Most importantly, just like a specific cognitive function is often linked to structural and functional features of a specific brain network or region, can we link the overall positive

feature of subject measures, varying along the “positive-negative” mode, to structural and functional features of any specific brain area or network?

Here we seek the answer to the above questions by studying the population covariation of three distinct modalities of data: cortical thickness (a morphometric brain property that has been repeatedly linked to various behavioral aspects), functional connectivity, and behavioral and demographic measures, in a large cohort of HCP subjects. We simply apply CCA to all pairs of the three modalities and find their maximal correlations are approximately aligned in the same “positive-negative” mode direction. More importantly, the overall negative-to-positive change of subject measures along this mode direction is associated with a similar divergent pattern of modulations in both cortical thickness and functional connectivity: the thinner cortex and increased functional connectivity at the higher-order brain regions in charge of more complex cognitive functions whereas the thicker cortex and reduced functional connectivity at the lower-order sensory/motor areas. Our present results are consistent with several previous studies to a large extent(Ly et al., 2012; Song et al., 2008), especially positive correlation between the functional connectivity at high-order regions and intelligence or cognition (Hampson et al., 2006; Langeslag et al., 2013; Song et al., 2008) and negative correlation between thickness at some high-order regions, such as frontal and parietal cortices, and high-level life satisfaction (Zhu et al., 2018) or intelligence quotient (IQ) (Choi et al., 2008). These results provide new insight into the three-way relationship among brain structure, brain activity, and human behavior by suggesting that the cross-hierarchy contrast between the lower-order unimodal regions (sensory and motor networks) and higher-order transmodal areas (mostly the default mode and frontal-parietal networks) (Jones and Powell, 1970; V azquez-Rodríguez et al., 2019), is the key feature, at least for both cortical thickness and functional connectivity, closely linked to a specific aspect, i.e., the overall positive feature, of human behavioral and demographic measures, and this relationship represents the maximal correlations found among the three modalities of data.

2. Materials and methods

2.1. Data and code availability statement

The demographic, behavioral measures, cortical thickness, and functional connectome data are from the HCP dataset (http://humanconnectome.org/data). All data is available in the main text or the supplementary files. The Matlab code in the present analysis is freely available at GitHub (https://github.com/fenghan1202/the_cca_project).

2.2. Ethics statement

The use of de-identified data from the HCP and the sharing of analysis results has been reviewed by the Pennsylvania State University Institutional Review Board and also strictly followed the HCP data use agreements.

2.3. Experimental design

We applied a data-driven canonical correlation analysis (CCA) to seek the maximal correlations and associated features between the three modalities of data, including the

functional connectivity measured with the resting-state fMRI signals, the cortical thickness assessed based on T1-weighted structural MRI, and 129 behavioral and demographic measures from a large-cohort of 818 subjects in the HCP.

2.4. Data and preprocessing steps

We used structural MRI and resting-state fMRI data from 818 HCP subjects. All subjects were healthy adults (28.8 ± 3.7 years old, 365 females), who underwent one imaging sessions of structural MRI (T1w_MPR1 series, 3D MPRAGE, TE = 2.14 ms, TR = 2400 ms, 0.7 mm spatial resolution) and 4 sessions of resting-state fMRI (15 min each, TE = 33.1 ms, TR = 720 ms, multiband acceleration factor of 8) scanning on a 3T Siemens connectome-Skyra scanner.

The functional and structural imaging data were preprocessed with the HCP minimal preprocessing pipelines (Van Essen et al., 2013). Briefly, structured artifacts were identified and removed for each resting-state fMRI run by independent component analysis (ICA) followed by FMRIB's ICA based X-noiseifier (Griffanti et al., 2014; Salimi-Khorshidi et al., 2014), which can remove 99% artifactual ICA components in each dataset. The resting-state fMRI data was mapped as time series of grayordinates, including cortical surface vertices and spatially standardized subcortical voxels. We obtained the resting-state functional connectivity of 200 distinct brain regions directly from the HCP PTN (Parcellation + Timeseries + Netmats) dataset (Smith et al., 2015), which is publicly available. Theþdataset includes the resting-state connectivity measures for brain parcels ("nodes") derived with the ICA at several different dimensionalities (50, 100, 200, 300). Following the previous study (Smith et al., 2015), we used the resting-state fMRI connectivity measure based on partial correlations (Marrelec et al., 2006) of 200 ICA parcels for all the results presented in the paper, and we also tested the results from different ICA parcels described as below. Notably, the use of full Pearson's correlations did not change the major results and thus the conclusions of this paper. Refer to the previous report (Smith et al., 2015) about details of deriving the ICA parcellations and associated resting-state fMRI connectivity measures. The preprocessing of the structural imaging includes the T1w and T2w images alignment, bias field correction, the volume space registration into MNI space, white and pial cortical surface reconstruction, which derived the cortical thickness over the entire neocortex. We further performed spatial smoothing (FWHM = 6 mm) on cortical thickness surface maps of 32K resolution.

2.5. CCA between cortical thickness and behavioral/demographic measures

We used the CCA method (Hotelling, 1936) to identify the maximal linear correlation between cortical thickness at all surface vertices and 129 behavioral/demographic measures. Each significant CCA mode identifies a linear combination of thickness measurements and a linear combination of behavioral/demographic measures, which are maximally correlated with each other across subjects. Specifically, thickness on the surface of 32K resolution (818 subjects × 59,412 vertices as matrix T_1) and 129 behavioral and demographic measures (from the original set of 478 measures, 818 subjects × 478 measures as S_1) were linked together using CCA.

We also generated an additional matrix T_2, where each column of T_1 was normalized according to its mean, and removed the badly conditioned columns with a low mean value (less than 0.1). Column-wise demeaning and matrix-wise variance-normalization were operated for $T_1$and T_2, respectively, and then those two resulting matrices were concatenated horizontally to give rise to a matrix T_3 that includes both preferences as the previous study (Smith et al., 2015). An inverse Gaussian transformation based on ranking was used to promote Gaussianity of S_1 and generate S_2, by which the effect from potential outliers would be decreased.

11 behavioral/demographic measures were considered as the confound factors:

1. Acquisition reconstruction software version.
2. Gender.
3. Age.
4. Mean head motion (van Dijk et al., 2012).
5. Weight.
6. Height.
7. Systolic blood pressure.
8. Diastolic blood pressure.
9. Blood hemoglobin A1C measures.
10. The cube-root of brain volume (ventricles included, estimated by FreeSurfer).
11. The cube-root of intracranial volume (estimated by FreeSurfer).

Besides those 11 measures, we demeaned and squared the measures 3–11 (since the first two are binary), and then took them as another set of confounding factors so that we can remove the potentially nonlinear effects of those measures. All 20 confound factors were demeaned and then regressed out from the $T_3$and S_2.

Race was excluded from the analysis similar to the previous study (Smith et al., 2015). Several subject measures were also excluded before CCA as described:

1. The 11 confound behavior measures listed above.
2. 88 poorly quantified measures according to the following criteria (Smith et al., 2015):
    a. Fewer than 250 subjects with valid measures;
    b. Measures that >95% of subjects had the identical scores;
    c. The measures had extreme outlier value. For x_s as the score of subject s for a subject measure, we calculated $y_s = (x_s - \text{median}(x_s))^2$. If $\max(y_s) > 100 \times \text{mean}(y_s)$, we regarded the measure as having extreme outliers.
3. 45 variables that are perceived irrelevant to brain function (For example, “Is the subject born in Missouri?” or “Is the subject in a live-in relationship?”) or highly

dependent variables (i.e. Body mass index is dependent on height and weight). All of those 45 variables are same to a previous study (Smith et al., 2015).

4. 191 imaging measures that are not behavioral traits (i.e. cortical thickness, regional volume and surface area).

5. 22 measures related to the alcohol use. Although the inclusion of alcohol measures produced very similar CCA results (Fig. S1), the alcohol usage exhibited similar correlations as positive personal traits with the cortical thickness and functional connectivity. Although the finding is consistent with their positive correlations with fluid intelligence, which were found in both the current study and previous ones (Belasen and Hafer, 2013), it is somewhat against the common perception of alcohol usage as a substance use. To avoid the complications, we excluded the measures related to alcohol use from the main analysis.

The above procedures gave rise to a 818 subjects × 129 subject measures matrix S_3. We list those 129 measures in Table S1. Importantly, the principal component analysis (PCA) was performed to reduce non-subject dimensions to 100, which is consistent with the previous study (Smith et al., 2015), in order to avoid overfitting in CCA. That is, the first 100 principal components of both subject measures and thickness (named T_4 and S_4, respectively, both were 818 × 100 in size) were used for thickness-behavior CCA. Notably, the T_4 and S_4 accounted for the 99.72% and 82.28% of the total variance of behavior and thickness data respectively. Moreover, other principal component numbers, such as 60, 80 and 120, were also applied to validate the reproducibility of the above CCA (Fig. S2).

The CCA, implemented by the Matlab function *canoncorr*, estimated 100 modes by optimizing the de-mixing matrices A_{TS} and B_{TS} to obtain the maximal similarity between the two matrices $U_{TS} = T_4 A_{TS}$ and $V_{TS} = S_4 B_{TS}$ (both were 818 × 100 and pair in size), each of corresponding columns from U_{TS} and V_{TS} represents the strength with which a mode of population variation is common to subject measures and thickness. For statistical inference, we permuted the index of subjects (the rows of T_4 or S_4) by 100,000 times without removing the family structure as previous study (Smith et al., 2015) (since the 818 HCP subjects are from hundreds of families) and run CCA for each permutation to build a null distribution (Fig. 1B).

The principal CCA mode was identified as the first pair of canonical variates with the highest correlation ($r = 0.70$, $p < 1.0 \times 10^{-5}$, corrected for multiple comparisons across all modes estimated), which was the only significant mode ($p < 0.05$) among all 100 modes. Multiple comparisons were corrected using the family-wise error rate (FWER) referred to the Matlab script provided by previous study (Smith et al., 2015). The canonical variates of this principal mode, i.e., the first columns of U_{TS} (818 × 1) and V_{TS} (818 × 1), were correlated with cortical thickness (818 × 59,412) and subject measures (818 × 478), respectively, and the resulting weights indicate the contributions of the cortical thickness at single vertices and individual subject measures to the identified CCA mode. The map of thickness correlations (thickness weights, 59,412 × 1) was further converted to Z score using

Fisher's transformation. The basic procedures of thickness-behavior CCA modeling is summarized as a diagram shown in Fig. S3.

To examine changes in cortical thickness along the direction of the identified CCA mode, we defined a CCA score for the identified CCA mode as the mean of the corresponding pair of canonical variates, i.e., the first columns of U_{TS} and V_{TS}. The 818 subjects were divided into four groups according to the quartiles of their CCA scores. We also defined two masks covering the lower (positively correlated with the principal CCA, $p < 0.05$, uncorrected, warm color portion in Fig. 1D) and higher (negatively correlated with the principal CCA mode, $p < 0.05$, uncorrected, cold color portion in Fig. 1D) hierarchical regions, respectively. The cortical thickness was averaged first within these two masks and then across subjects within each of the four groups to show the divergent modulations of cortical thickness across the cortical hierarchy along the identified CCA mode (Fig. 1E).

We also examined the relationship between the cortical thickness at the higher- and lower-order regions. We first calculated the mean thickness at the higher- and lower-order masks for each subject and showed their association across individuals. We then repeated this procedure for the cortical thickness normalized by the mean over the entire cortex, which removed the large inter-subject variability in the mean cortical thickness. The control masks were constructed by rotating the higher- and lower- order masks with random degrees and then the relationship of the normalized cortical thickness in these pairs of control masks was also examined (Fig. S4).

To make sure that the overall relationship between the thickness and behavior is not due to any single or specific category of subject measures, we employed a leave-one-out procedure to re-run the CCA with excluding one of 129 subject measures or one of ten categories each time. We also derived the cortical thickness weights (59,412 × 1) for each reduced principal CCA mode and then correlated these 129 thickness weights results (59,412 × 129) (or 10 thickness weights (59,412 × 10) from "leave-one-category-out") with thickness weights derived from the original one without leave-one-out (59,412 × 1) (Fig. S5B–C). In addition, we also directly correlated 8 leading subject measures (818 × 8, 8 subject measures showing the strongest correlations (absolute value) in Fig. 1C) with the cortical thickness measures (818 × 59,412) across 818 subjects (Fig. S5D–K) to derive the thickness weights for each of these 8 subject measures.

We demonstrated the reproducibility of the thickness-behavior CCA and confirmed that the results are not from any specific subject with a split-half test. To be specific, we replicated our analysis on two randomly split samples (each was in a size of 409 subjects) and then obtained the spatial patterns of (Fisher) z-transformed thickness weights for both first and second half group shown as Fig. S6.

To test whether the cross-hierarchy contrast of the cortical thickness is more closely related with the subject measures than region-based measures, we calculated the mean cortical thickness within the lowand high-hierarchy masks shown in Fig. 1D and E, as well as their ratio, and then correlated them (818 × 3) with 129 subject measures across all 818 subjects (818 × 129). The resulting correlations were sorted and compared with those derived using

the mean cortical thickness of 66 predefined brain regions (Desikan et al., 2006). To build a control case for the ratio index, we rotated the two masks on the spherical brain surface by randomly generated angles ([294, 327, 46] with respect to the x, y and z axis respectively). We then calculated the mean cortical thickness within the control masks and their ratio, and correlated the thickness ratio between the control masks with the behavioral/demographic measures. Each group of correlations results (from the 5 sets) was sorted based on their correlation coefficients (Fig. 2A). We then counted the number of significantly correlated ($p < 0.05$, uncorrected) subject measures for each of four different thickness measures, including the mean thickness of the low-hierarchy mask, of the high-hierarchy mask, the thickness ratio between the low- and high-hierarchy masks, and between the two control masks (Fig. 2B). For subject measures showing significant correlations with more than one thickness measure, we compared their absolute correlations with a pair of thickness measures using scatter plots (Fig. 2C). To avoid circuity, we defined new lower- and higher-order masks based on the first half results of thickness weights and replicated the above analysis by comparing various thickness measures (within the new masks) in terms of their correlations with subject measures (Fig. S7).

To examine whether the CCA simply links the main feature dimensions of the unimodal-transmodal axis for the thickness and the positive-negative axis for the subject measures. We examined the correlation between identified CCA mode and the first 100 principal components of the two modalities of data, respectively (Fig. S8).

2.6. CCA between functional connectivity and behavioral/demographic measures

We replicated the connectome-behavior CCA (Smith et al., 2015) for 818 subjects. Functional connectivity data was obtained from PTN dataset described above. To be specific, the Netmat from 200-dimensional group-ICA was used as the connectivity matrix. The 200 × 200 Netmat matrices give functional connectivity (partial correlations converted to Z scores already) for 19,900 pairs (upper triangular matrix without diagonals) of brain regions. Matrices of functional connectivity (C_1, 818 × 19,900) and subject measures (S_1, 818 × 129) were constructed for all the subjects. To make sure the functional connectivity is free from the head motion after we regressed out the mean motion as a confounding factor, we correlated the C_1 with another head motion index, the mean framewise displacement (FD) averaged over a session, across 818 individuals, and 0 out of the 19,900 pairwise connections was significantly correlated ($p < 0.05$, uncorrected). Using the same procedures described above, we performed CCA and obtained a highly significant connectome-behavior CCA mode ($r = 0.77$, $p < 1.0 \times 10^{-5}$, corrected for multiple comparisons). We also correlated the corresponding canonical variates in this significant (principal) CCA mode, i.e., the first columns of U_{CS} and V_{CS}, with the original sets of connectivity C_1 and subject measures S_1 respectively and obtained the connectivity weights A_{CS} and behavior weights B_{CS} to show how the connectome-behavior CCA mode is correlated with functional connection between each pairwise brain regions and single subject measure. Since the connectivity metric can be negative values, its negative correlation with the CCA canonical variate may actually indicate as a decrease of connectivity strength along the direction of CCA mode. We thus multiplied each connectivity weight, i.e., the correlation between single connectivity and the CCA canonical variate, by the sign of population mean connectivity

(averaged C_1 across each column), and the results quantify how the strength (i.e., amplitude) of single functional connectivity is correlated with the identified CCA mode. Then, we mapped the connectivity strength modulations (along the CCA direction) onto the brain surface by counting, for each brain parcel, the number of connections (out of 199 in total) showing significantly positive (increased connectivity strength with increased CCA scores) and negative (decreased connectivity strength with increased CCA scores) correlations with the CCA connectivity canonical variate (Fig. 3A and B). The resulting "connectivity strength decrease" map was also subtracted from the "connectivity strength increase" map to derive a "difference" map for functional connectivity modulations (Fig. 3C), whose map scores were averaged within the higher- and lower-hierarchy masks respectively. This parcel-based mapping method is modified based on the previous one, which multiplied the functional connectivity strength modulation of each ROI with its spatial ICA map and then summed them up to obtain a final map. Although the previous approach gives a smooth transition across the cortex, we found that the resulting maps all share a spatial pattern with the simple summation of all the ICA maps (Fig. S9).

To increase confidence that the connectome-behavior CCA mode is robust, we replicated the CCA on the same subject measures and Netmat (connectivity) derived from 50-, 100- and 300-dimensional group-ICA parcellation respectively. Similar to the previous study (Smith et al., 2015), we examined the following correlations between the original mode (200-dimensional ICA parcellation) and the alternative one:

1. The connectivity variates in principal CCA mode (the most significant one with maximal correlation): Ucs_1(original) versus Ucs_1(alternative);
2. The behavior variates in principal CCA mode: Vcs_1(original) versus Vcs_1(alternative);
3. The behavior weights derived by the principal CCA mode: Bcs(original) versus Bcs(alternative);

The connectivity weights Acs was excluded in the comparison due to incompatible dimensions between the original and alternative one. We thus obtained the above three correlations between the original mode and the 50-dimensional one as [0.56 0.75 0.88], the 100-dimensional one as [0.63 0.82 0.93] or the 300-dimensional one as [0.60 0.81 0.94] (all p-values $< 2.45 \times 10^{-67}$, uncorrected).

2.7. CCA modeling of cortical thickness and functional connectivity

Using the same procedures as the other two CCA modeling, we applied the CCA to the thickness data and Netmat from 200-dimensional group-ICA (200 × 200) to derive thickness-connectivity CCA modes. This produced 8 significant CCA modes in which the first one had the highest correlation ($r = 0.80$, $p < 1.0 \times 10^{-5}$). We also correlated local cortical thickness and pairwise functional connections to the first CCA mode, i.e., the corresponding canonical variates, to obtain the canonical weights for both modalities (Fig. 4 D and 4E).

2.8. Eigen direction for the population covariance of three modalities

We performed PCA on the 6 canonical variates from the three CCA modes and took the first principal component (explains 64.93% of the total variance) as an eigen-direction of population covariance of these three modalities of data. We validated this eigen-direction by correlating it with these 6 canonical variates from three principal CCA modes. We also computed the correlation between the two behavioral weights from principal thickness-behavior CCA mode and principal connectome-behavior CCA mode, the correlation between the two thickness weights from principal thickness-behavior CCA mode and principal thickness-connectome CCA mode, and the correlation between the two connectome weights from principal connectome-behavior CCA mode and principal thickness-connectome CCA mode (Fig. 4).

It is worth noting that CCA can result in strong correlations even for permutated cases that are not supposed to have any relationship. To control this effect on the result of the eigen-direction, we adapted a similar approach of permutation tests we used to infer the significance of the CCA modes. We repeated the entire eigen-direction analysis for the control CCA modes obtained for the permuted cases. For each of these permuted cases (N = 10,000), the correlations between the eigen-direction and 6 individual canonical variates were averaged for each case to build a null distribution, which was then compared with the real case without permutation (Fig. S10).

To cross-validate the result of eigen-direction analysis, we also applied a generalized canonical correlation analysis (gCCA) (Smilde et al., 2017) to assess the three-way relationship among the cortical thickness, connectome and subject measures. We used the gCCA toolbox (https://nofimamodeling.org/software-downloads-list/pca-gca-toolboxfor-matlab/) to achieve this goal. The three modalities of data went through the identical pre-processing as the pairwise CCA before they were fed into the gCAA toolbox, and the PCA dimension for the gCCA was also set to 100 in order to keep consistent with the pairwise CCA.

2.9. Statistical analysis

We used permutation tests to determine the statistical significance of the identified CCA mode. Specifically, to test the significance of identified CCA modes, we permuted the index of subjects for 100,000 times to disrupt the correspondence between modality pairs without removing the family structure, and then ran CCA on permuted data to build a null distribution for CCA correlations (Fig. 1B). In addition, we controlled the FWER to address multiple comparison problem. We used the Pearson's correlations to quantify the degree of association, i.e., the canonical weights, between the identified CCA mode and each of relevant modalities. We then transformed these correlation coefficients to Z scores using Fisher's transformation and determined the significance of the weights according to the Z scores (Fig. 1D). We applied the leave-one-out procedure for the thickness-behavior CCA to validate that the major effect of cortical thickness changes across subjects was linked to the whole set of behavioral measures rather than dominated by some specific ones (Fig. S5). The reproducibility of the thickness-behavior CCA was verified with a split-half test. To be specific, we randomly split samples into two halves (409 subjects for each), replicated the

thickness-behavior CCA on these two sub-groups of subjects respectively and then examined the spatial pattern of the cortical thickness weights for both groups (Fig. S6). For the identified connectome-behavior mode, two sample *t*-test was used to compare the difference of the functional connectivity strength modulations between the high-order cortices and the low-order ones (Fig. 3D). Besides, the Pearson's correlation was also employed to compare the associations between 6 canonical variates from the three CCA modes and their eigen-direction (middle panel in Fig. 4), and the similarities between corresponding canonical weights from different CCA modes, such as two behavior weights from the identified thickness-behavior and connectome-behavior CCA modes (Fig. 4A and B). Likewise, we transformed these correlation coefficients to Z scores and made statistical inference accordingly. In this study, a p-value less than 0.05 was regarded as statistical significance.

3. Results

We used multimodal data from 818 HCP subjects who have completed all four resting-state fMRI sessions. We summarized the cortical thickness over the entire cortex (59,412 vertices), resting-state functional connectivity among 200 distinct brain regions (19,900 connections) parceled with independent component analysis (ICA) (Comon, 1994), and 129 non-imaging behavioral and demographic measures (we refer to as subject measures thereafter) for all the subjects. We then applied CCA, a procedure to seek maximal correlations and corresponding linear combinations of any two sets of variables, to all pairs of the three modalities of data after regressing out potential confounds (including age, gender, head motion, brain size, height, weight, blood glucose level, and blood pressure) and reducing non-subject dimension to 100 using the principal component analysis (PCA) (Pearson, K., 1901). All the procedures above were adapted from the previous study that identified the positive-negative CCA mode between the functional connectivity and behavioral/demographic measures (Smith et al., 2015).

3.1. The maximal thickness-behavior correlation is associated with characteristic changes of both modalities

The application of CCA to the cortical thickness and behavioral data revealed a single highly significant ($r = 0.70$, $p < 1.0 \times 10^{-5}$, corrected for multiple comparisons across all modes estimated, Fig. 1A and B) mode that represents the maximal correlation between the two. The canonical weights of behavioral measures, i.e., the correlations between single subject measures and the behavior canonical variate, show a pattern similar to what has been found for the connectivity-behavior CCA mode (Smith et al., 2015): the subject measures commonly considered as positive traits, e.g., the fluid intelligence and life satisfaction, are positively correlated with the CCA mode whereas the measures of negative traits, e.g., marijuana use and behavioral aggression, tend to show negative correlations (Fig. 1C). In fact, the most strongly correlated subject measures, particularly those positive traits, are overlapped with those showing the top correlations with the connectivity-behavior mode, including the vocabulary scores, fluid intelligence, life satisfaction, and tobacco use (Smith et al., 2015). In summary, the cortical thickness co-varies maximally with the behavioral/demographic measures in a direction also featuring the positive-negative behavioral change.

More interestingly, the canonical weights of the cortical thickness, i.e., the correlations of local cortical thickness (at single vertices) with the identified thickness-behavior CCA mode, revealed a striking spatial pattern of divergent modulations across cortical hierarchy (Fig. 1D). Specifically, significant positive correlations are seen mostly at lower-order sensory/motor areas, including the sensorimotor, auditory, and visual cortices, whereas strong negative correlations appear mostly at higher-order brain regions, including the frontal, anterior temporal, and parietal cortices that encompass the most parts of the default mode network (DMN). The contrast is evident across hierarchies in the neocortex, even though positive correlations are also seen at some parts of the allocortex and mesocortex, such as the hippocampal formation and olfactory bulb. In other words, towards one end of this CCA mode individuals tend to show more positive subject traits, thinner cortex at the higher-order cortical regions, but thicker cortex at the lower-order sensory regions (Fig. 1E). It is worth noting that Fig. 1E shows the modulation of the cortical thickness along the CCA mode direction. The opposite modulations of thickness in the higher-order and lower-order regions along this particular direction do not imply a negative correlation between the two, which can only be seen with controlling the mean cortical thickness (Fig. S4). The thickness-behavior relationship is not driven by any specific, or any specific group of, subject measures since leaving any one of them out of the analysis produced almost no changes in the final results. Moreover, single subject measures show much weaker correlations with the cortical thickness, which do not show any noticeable pattern of cross-hierarchy divergence (Fig. S5). We also conducted a split-half reliability test by randomly dividing subjects into two halves (409 subjects for each) and repeating the CCA analysis on both groups. Similar results, particularly the spatial pattern of cortical thickness weights, were obtained on both groups even with reduced statistical power (Fig. S6).

3.2. Cross-hierarchy contrast of the cortical thickness is tightly linked to behavioral measures

The above results imply that the cortical thickness difference between the lower- and higher-order brain regions could be more closely linked to subject measures than region-based statistics. To test this hypothesis, we compared the cross-hierarchy contrast and region-specific cortical thickness in terms of their correlation with behavioral/demographic measures. In addition to the cortical thickness ratio between the lower-and higher-order regions, we calculated the mean cortical thickness of 66 predefined regions (Desikan et al., 2006), of the lower- and higher-order regions, and the cortical thickness ratio between two sets of control brain regions, which were obtained by randomly rotating the masks for the lower- and higher-order brain regions on the brain surface. Compared with the other thickness measures, the cortical thickness ratio between the lower- and higher-order regions showed much stronger correlations with the subject measures (Fig. 2A and B). In addition, the correlation strength is consistently higher for this cross-hierarchy thickness ratio than any other thickness measures for any subject measures showing significant correlation to both (Fig. 2C). In summary, the cross-hierarchy contrast of cortical thickness appears to be a feature more tightly coupled with the overall subject measures than any region-based measures.

It is worth noting that the above results presented information overlapped with the findings from the thickness-behavior CCA mode (Fig. 1), and was intended more for a quantitative comparison between the cross-hierarchy contrast and region-based measures of thickness in terms of their relationship with behavioral data. To avoid the circularity, we repeated the same analysis using the two groups of subjects from the split-half test (Fig. S6). The data from the first group was used as a test set for defining the lower- and higher-order regions using the CCA analysis, and the second half of the data was then used as a validation set to compare various thickness measures in terms of their correlations with subject measures. Similar results were obtained (Fig. S7).

3.3. Co-modulations of functional connectivity with behavior show a cross-hierarchy contrast

Given the negative-to-positive behavioral change along the thickness-behavior CCA mode is similar to what has been observed for the connectivity-behavior CCA mode (Smith et al., 2015), we wanted to know whether the functional connectivity modulation along the connectivity-behavior CCA mode shares any similar features with the cortical thickness modulation along the thickness-behavior CCA mode. Towards this goal, we first applied CCA to the functional connectivity and behavioral data from 818 HCP subjects. Consistent with the previous study (Smith et al., 2015), we found a single highly significant the CCA mode ($r = 0.77$, $p < 1.0 \times 10^{-5}$, corrected) between the two modalities, which shows opposite correlations with positive and negative subject traits (Fig. S11). The top ones are largely overlapped with those of the thickness-behavior CCA mode (Fig. 1C).

We then examined the modulation of functional connectivity along this connectivity-behavior CCA mode. Briefly, we identified functional connections, among those of the 200 brain regions, that are significantly modulated along the connectivity-behavior CCA mode, i.e., showing significant correlation ($p < 0.05$, uncorrected) with the connectivity-behavior CCA mode. These connections are then multiplied by its sign to quantify how much their strength is upregulated (i.e., the positive connectivity becomes more positive or negative ones become more negative) or downregulated along the CCA mode direction. For each brain region, we counted the numbers of significantly upregulated and downregulated connections respectively and mapped the results onto the brain surface (Note: one brain region has both upregulated and down-regulated connections). It should be noted that the mapping was done based on parcels rather than the ICA maps of the 200 regions (Smith et al., 2015), because the ICA maps can introduce a strong spatial pattern regardless of the connectivity changes (Fig. S9). The two resulting maps represent the degree to which the overall functional connectivity strength changes (increase or decrease) towards high-scoring subjects with more positive traits. A cross-hierarchy contrast is evident in both maps but in an opposite manner. The higher-order regions, particularly DMN, showed the largest degree of connectivity strength increase but the smallest degree of connectivity strength decrease, whereas the lower-order sensory/motor areas had an opposite pattern of modulation (Fig. 3A and B). The cross-hierarchy pattern of the functional connectivity modulation is even clearer in the difference between the two maps (Fig. 3C).

3.4. A single direction featuring the maximal population covariation of the three modalities

The connectivity-behavior mode and thickness-behavior mode showed strong correlations with a similar set of subject measures (Fig. 1C and Fig. S11). In addition, the modulation of functional connectivity and cortical thickness along the two CCA modes displayed a similar divergent pattern across the cortical hierarchy (Figs. 1D and 3C). These correspondences suggest that the two modes may actually represent a similar direction in the subject space, which might also mediate the maximal correlation between the functional connectivity and cortical thickness. To have a complete understanding of the population covariation of the three modalities, we performed CCA between the functional connectivity and cortical thickness. Eight pairs of canonical variates survived through the statistical test ($p < 0.05$, corrected). The first pair with the highest correlation and the most significant p-value ($r = 0.80$, $p < 1.0 \times 10^{-5}$, corrected) is associated with similar divergent modulations of both functional connectivity and cortical thickness (Fig. 4), suggesting it is closely related to the other two CCA modes. The 6 canonical variates from the three pairs of CCA show strong correlations with each other (correlation coefficients: 0.58 ± 0.13, all $p < 7.5 \times 10^{-36}$). We then performed PCA on the 6 canonical variates to obtain the first principal component to represent an eigen-direction of the population covariation of the three modalities (Fig. S10). This eigen-direction accounts for 64.93% of the total variance of these 6 canonical variates and is highly correlated with each of them (correlation coefficients ranging from 0.78 to 0.82, all $p \leq 9.37 \times 10^{-170}$) (Fig. 4). To cross-validate the eigen-direction result, we also applied a generalized canonical correlation analysis (gCCA) to quantify the three-way covariation of the three modalities (Smilde et al., 2017), and a strong three-way correlation ($r = 0.7$) was found among them. Overall, the findings suggest that the population variations of the cortical thickness, functional connectivity, and behavioral/demographic measures are maximally linked to each other along a similar direction in the subject space that is featured by an increase of overall positive feature of subject measures and a divergent modulation of both functional connectivity and cortical thickness at the higher-order brain regions and low-level sensory/motor areas.

4. Discussions

By applying a data-driven CCA to the cortical thickness, resting-state functional connectivity, and demographic/behavioral measures from a large cohort of subjects, we found that the maximal thickness-behavior correlation and the maximal connectivity-behavior correlation are converged in a specific direction, along which all three modalities show very characteristic modulations. Towards one end of this direction, individuals tend to have more positive subject traits as described previously (Smith et al., 2015), but more importantly, their functional connectivity and cortical thickness show a similar divergent modulation across the cortical hierarchy, i.e., increased functional connectivity and thinner cortex in the higher-order brain regions whereas decreased connectivity and thicker cortex at the low-level sensory/motor areas. Modern neuroimaging has been successful in linking specific aspects of brain function and/or human behavior to specific brain networks/regions. Based on the findings in this study, we argue that structural and functional contrast between the lower- and higher-order brain regions might be the brain feature tightly linked to a

specific behavioral dimension that quantifies the overall positive feature of human behavior and demographics.

The lower- and higher-order cortical regions showing opposite modulation in our CCA results are known to be structurally and functionally distinct. The higher-order brain regions expand much more as the brain size increases (Reardon et al., 2018), over the developmental course (Hill et al., 2010), and also across species from monkeys to humans (Hill et al., 2010). In contrast, the lower-order sensory regions have a higher level of cortical differentiation and thus more refined layers (Braak et al., 2017). Cortical myelination follows a trajectory from the lower-order regions to the higher-order regions and thus creates a strong contrast between the two, which can be readily assessed by MRI-derived T1-weighted/T2-weighted maps (Glasser and Van Essen, 2011). These structural differences, as well as other known differences in cytoarchitecture, cell types, and synaptic physiology (Burt et al., 2018), between the two sets of brain regions are consistent with their distinct gene expression profiles (Burt et al., 2018; Reardon et al., 2018). Altogether, they may serve as the basis of their distinct functions, including those seen with neuroimaging tools. For example, embedding resting-state functional connectivity matrix into a low-dimensional space revealed a principal gradient separating the lower-order sensory/motor regions from the higher-order DMN (Margulies et al., 2016). A meta--analysis of numerous neuroimaging literature identified a functional spectrum along this hierarchical gradient from simple sensory perceptions to abstract and complex cognitive functions (Margulies et al., 2016). A series of studies have found consistent evidence across species that the resting-state connectivity/dynamics are divergently modulated across the lower- and higher-order regions from wake to anesthetized conditions (Barttfeld et al., 2015; Liang et al., 2015; Ma et al., 2017; Martuzzi et al., 2010). In addition, resting-state fMRI connectivity changes associated with a general psychopathological score, which reflects chronicity and symptom severity of mental illness in patient groups but risks in healthy individuals, also diverge in these two sets of brain regions (Elliott et al., 2018). It has been found that the correlation between functional connectivity and behavioral measures is partly due to the inter-subject variability in the spatial arrangement of functional networks (Bijsterbosch et al., 2018). This is likely also a factor contributing to the connectivity-behavior correlations observed in our study, and may also explain the good spatial correspondence between the connectivity and thickness modulations along the positive-negative behavioral axis.

The cortical thickness has been linked to various aspects of the human behavior, particularly the human intelligence (also seen in Fig. 1A), measured either with the intelligent quotient (IQ) or a general intelligence g-factor quantifying more general cognitive capabilities, by multiple studies (Choi et al., 2008; Colom et al., 2009; Fjell et al., 2015; Karama et al., 2011; Narr et al., 2007). Most of them reported a positive association between the cortical thickness and intelligence. Although the spatial pattern of correlations varied across studies, relatively consistent correlations were observed in the lower-order sensory/motor regions (Choi et al., 2008; Colom et al., 2009; Karama et al., 2011; Spearman, 1904). The overall thickness-behavior correlations in the present study (Fig. 1D) biased slightly towards positive, which is somewhat consistent with the previous observations. However, significant negative correlations between the intelligence and the cortical thickness of higher-order brain regions were largely absent in the existing literature. There could be multiple reasons.

First, the set of subject measures we used include real-life functions and demographic measures, such as education, income and life satisfaction, which can contribute significantly to the identified CCA modes. Indeed, the cortical thinning has been observed at the higher-order brain regions, including the middle and superior frontal gyrus, in subjects with a high level of life satisfaction (Zhu et al., 2018), as well as at the primary sensory/motor areas in adults with psychopathy or violent antisocial personality disorder (Ly et al., 2012; Narayan et al., 2007) or school children showing aggressive behaviors (Thijssen et al., 2015). These findings are to a large extent in accordance with the divergent changes of the cortical thickness we found here. However, the contribution of the life-related factors cannot explain significant negative correlations between the thickness at some higher-order cortices, such as the frontal regions, and single measures of fluid intelligence or picture vocabulary (Fig. S5D–F). Thus, the discrepancy might also be due to other factors, such as differences in the cohort size, data quality, and pre-processing algorithms. In addition, a dynamic thickness-intelligence relationship across the lifespan and the relatively young age (28.8 ± 3.7 years old) of the HCP subjects might also contribute to this discrepancy (Schnack et al., 2015).

Neural mechanisms underlying the divergent modulation of the cortical thickness are unclear, but there are a few possibilities based on previous literature. The cortical thinning is a process featuring the developmental course and has been hypothesized to reflect a neuronal pruning process of removing inefficient synapses (Fjell et al., 2015; Kanai and Rees, 2011). In addition, intracortical myelination can also result in the apparent thinning of the MRI-reconstructed cortex (Fjell et al., 2015). These microstructural changes might underlie the association between positive subject traits and the thinning of the higher-order cortex. In contrast, other region-specific processes may be involved in determining the thickness of the primary sensory/motor cortices, which showed an opposite modulation in the present study and much less significant change across the lifespan compared with the higher-order brain regions (Fjell et al., 2015). As an example, the loss of mirror neurons has been proposed to be a possible reason for the thinner primary motor cortex associated with aggressive and violent behaviors (Dushanova and Donoghue, 2010). However, these explanations remain conjectures before proven.

The present study has a few limitations. First, this is a purely correlative study and the caution should be exercised when one attempts to infer any causal relationships based on the results. For example, the divergent modulations across the cortical hierarchy along the CCA mode direction were observed both for the cortical thickness and functional connectivity. A parsimonious interpretation would be that the structural difference leads to functional changes. However, we should not exclude the possibility that spontaneous brain activity underlying the resting-state functional connectivity may help to shape brain structure and morphology, such as the cortical thickness. Secondly, the divergent cortical thickness modulations at the lower- and higher-order brain regions might be, to some degree, disassociated in subpopulations. The cortical thickening at the lower-order sensory/motor regions is more prominent in subjects with more negative traits, whereas the cortical thinning at the higher-order regions appears to be stronger at the other end of the CCA mode (Fig. 1E). Moreover, although the cross-hierarchy ratio of thickness showed much stronger correlations with single subject measures than region-based thickness measures (Fig. 2A), the overall correlation strength is relatively weak. A possible explanation is that the cortical

thickness is not a structural feature that can be linked to any single type of behavior. Thirdly, our analysis was focused on a single structural imaging modality of cortical thickness, which has been repeatedly linked to human behaviors by previous studies (Choi et al., 2008; Colom et al., 2009; Karama et al., 2011; Ly et al., 2012; Narayan et al., 2007; Thijssen et al., 2015; Zhu et al., 2018), and this represents a limitation as compared with a recent comprehensive study linking various structural modalities to behavioral measures (Llera et al., 2019). However, our study has its advantages by revealing that the maximal thickness-behavior correlation and connectivity correlation are largely aligned along the same direction and show a similar spatial contrast between the lower- and higher-order brain regions. Lastly, we excluded behavioral measures of alcohol use in our CCA models, because we are not sure whether the alcohol use in the HCP subject cohort should be regarded as a positive (Corrao et al., 2000; Müller et al., 2013) or negative (Grønbæk, 2009) subject trait. Our preliminary analysis also suggests that alcohol use is positively correlated with the CCA mode and other positive traits, such as fluid intelligence, which is against the common perception of it as substance use. However, the inclusion of the measures of alcohol use produced little effects on our overall results, particularly the divergent pattern of cortical thickness modulations (Fig. S1).

In summary, the cortical thickness, functional connectivity, and behavioral/demographic measures from a large cohort of 818 HCP subjects show maximal correlations with each other along a similar direction across individuals, indicating a convergence of cross-modality relationships among these three types of data. This mode direction is associated with characteristic modulations in all three modalities, including a change in the overall positive feature of behavioral and demographic measures and divergent modulations of both cortical thickness and functional connectivity across the cortical hierarchy between the lower-and higher-order brain regions. These findings suggest that the cross-hierarchy contrast of brain structural and functional properties may be an important feature tightly linked to a specific aspect, i.e., the overall positive feature, of human behavior and demographics.

Supplementary Material

Refer to Web version on PubMed Central for supplementary material.

Acknowledgments

This work was supported by the National Institutes of Health Pathway to Independence Award (K99/R00 5R00NS092996-03).

In addition, data were provided by the Human Connectome Project, WU-Minn Consortium (Principal Investigators: David Van Essen and Kamil Ugurbil; 1U54MH091657) funded by the 16 NIH Institutes and Centers that support the NIH Blueprint for Neuroscience Research; and by the McDonnell Center for Systems Neuroscience at Washington University. We are grateful for all researchers who make efforts on collecting and sharing this dataset to the present study.

References

Barttfeld P, Uhrig L, Sitt JD, Sigman M, Jarraya B, Dehaene S, 2015 Signature of consciousness in the dynamics of resting-state brain activity. Proc. Natl. Acad. Sci. Unit. States Am 10.1073/pnas.1418031112.

Belasen A, Hafer RW, 2013 Intelligence IQ and alcohol consumption : international data. Intelligence 41, 615–621. 10.1016/j.intell.2013.07.019.

Bijsterbosch JD, Woolrich MW, Glasser MF, Robinson EC, Beckmann CF, Van Essen DC, Harrison SJ, Smith SM, 2018 The relationship between spatial configuration and functional connectivity of brain regions. Elife. 10.7554/eLife.32992.

Biswal B, Zerrin Yetkin F, Haughton VM, Hyde JS, 1995 Functional connectivity in the motor cortex of resting human brain using echo-planar mri. Magn. Reson. Med 10.1002/mrm.1910340409.

Braak H, Rüb U, Schultz C, Tredici K Del, 2017 Vulnerability of cortical neurons to Alzheimer's and Parkinson's diseases. J. Alzheimer's Dis 10.3233/jad-2006-9s305.

Bullmore E, Sporns O, 2009 Complex brain networks: graph theoretical analysis of structural and functional systems. Nat. Rev. Neurosci 10, 186–198. 10.1038/nrn2575. [PubMed: 19190637]

Burt JB, Demirtaş M, Eckner WJ, Navejar NM, Ji JL, Martin WJ, Bernacchia A, Anticevic A, Murray JD, 2018 Hierarchy of transcriptomic specialization across human cortex captured by structural neuroimaging topography. Nat. Neurosci 21 10.1038/s41593-018-0195-0.

Choi YY, Shamosh NA, Cho SH, DeYoung CG, Lee MJ, Lee J-M, Kim SI, Cho Z-H, Kim K, Gray JR, Lee KH, 2008 Multiple bases of human intelligence revealed by cortical thickness and neural activation. J. Neurosci 28, 10323–10329. 10.1523/JNEUROSCI.3259-08.2008. [PubMed: 18842891]

Colom R, Haier RJ, Head K, Álvarez-Linera J, Quiroga MÁ, Shih PC, Jung RE, 2009 Gray matter correlates of fluid, crystallized, and spatial intelligence: testing the P-FIT model. Intelligence 37, 124–135. 10.1016/j.intell.2008.07.007.

Comon P, 1994 Independent Component Analysis, A New Concept ?*, vol. 36, pp. 287–314.

Corrao G, Rubbiati L, Bagnardi V, Zambon A, Poikolainen K, 2000 Alcohol and coronary heart disease: a meta-analysis. Addiction. 10.1046/j.1360-0443.2000.951015056.x.

Desikan RS, S egonne F, Fischl B, Quinn BT, Dickerson BC, Blacker D, Buckner RL, Dale AM, Maguire RP, Hyman BT, Albert MS, Killiany RJ, 2006 An automated labeling system for subdividing the human cerebral cortex on MRI scans into gyral based regions of interest. Neuroimage. 10.1016/j.neuroimage.2006.01.021.

Dohmen T, Falk A, Fliessbach K, Sunde U, Weber B, 2011 Relative versus absolute income, joy of winning, and gender: brain imaging evidence. J. Publ. Econ 10.1016/j.jpubeco.2010.11.025.

Dushanova J, Donoghue J, 2010 Neurons in primary motor cortex engaged during action observation. Eur. J. Neurosci 31, 386–398. 10.1111/j.1460-9568.2009.07067.x. [PubMed: 20074212]

Elliott ML, Romer A, Knodt AR, Hariri AR, 2018 A connectome-wide functional signature of transdiagnostic risk for mental illness. Biol. Psychiatr 10.1016/j.biopsych.2018.03.012.

Fjell AM, Grydeland H, Krogsrud SK, Amlien I, Rohani DA, Ferschmann L, Storsve AB, Tamnes CK, Sala-Llonch R, Due-Tønnessen P, Bjørnerud A, Sølsnes AE, Håberg AK, Skranes J, Bartsch H, Chen C-H, Thompson WK, Panizzon MS, Kremen WS, Dale AM, Walhovd KB, 2015 Development and aging of cortical thickness correspond to genetic organization patterns. Proc. Natl. Acad. Sci. Unit. States Am 112, 15462–15467. 10.1073/pnas.1508831112.

Glasser MF, Van Essen DC, 2011 Mapping human cortical areas in vivo based on myelin content as revealed by T1- and T2-weighted MRI. J. Neurosci 31, 11597–11616. 10.1523/JNEUROSCI.2180-11.2011. [PubMed: 21832190]

Goldstein RZ, Volkow ND, 2011 Dysfunction of the prefrontal cortex in addiction: neuroimaging findings and clinical implications. Nat. Rev. Neurosci 12, 652–669. 10.1038/nrn3119. [PubMed: 22011681]

Griffanti L, Salimi-Khorshidi G, Beckmann CF, Auerbach EJ, Douaud G, Sexton CE, Zsoldos E, Ebmeier KP, Filippini N, Mackay CE, Moeller S, Xu J, Yacoub E, Baselli G, Ugurbil K, Miller KL, Smith SM, 2014 ICA-based artefact removal and accelerated fMRI acquisition for improved resting state network imaging. Neuroimage 95, 232–247. 10.1016/j.neuroimage.2014.03.034. [PubMed: 24657355]

Grønbæk M, 2009 The positive and negative health effects of alcohol- and the public health implications. J. Intern. Med 10.1111/j.1365-2796.2009.02082.x.

Hampson M, Driesen NR, Skudlarski P, Gore JC, Constable RT, 2006 Brain connectivity related to working memory performance. J. Neurosci 10.1523/JNEUROSCI.3408-06.2006.

Hill J, Inder T, Neil J, Dierker D, Harwell J, Van Essen D, 2010 Similar Patterns of Cortical Expansion during Human Development and Evolution, vol. 107, pp. 13135–13140. 10.1073/pnas.1001229107.

Honey CJ, Sporns O, Cammoun L, Gigandet X, Thiran JP, Meuli R, Hagmann P, 2009 Predicting human resting-state functional connectivity from structural connectivity. Proc. Natl. Acad. Sci. Unit. States Am 10.1073/pnas.0811168106.

Hotelling H, 1936 Relations between two sets of variates. Biometrika. 10.2307/2333955.

Huntenburg JM, Bazin PL, Goulas A, Tardif CL, Villringer A, Margulies DS, 2017 A systematic relationship between functional connectivity and intracortical myelin in the human cerebral cortex. Cerebr. Cortex 27, 981–997. 10.1093/cercor/bhx030.

Jones EG, Powell TPS, 1970 An anatomical study of converging sensory pathways within the cerebral cortex of the monkey. Brain. 10.1093/brain/93.4.793.

Kanai R, Rees G, 2011 The structural basis of inter-individual differences in human behaviour and cognition. Nat. Rev. Neurosci 12, 231–242. 10.1038/nrn3000. [PubMed: 21407245]

Karama S, Colom R, Johnson W, Deary IJ, Haier R, Waber DP, Lepage C, Ganjavi H, Jung R, Evans AC, 2011 Cortical thickness correlates of specific cognitive performance accounted for by the general factor of intelligence in healthy children aged 6 to 18. Neuroimage 55, 1443–1453. 10.1016/j.neuroimage.2011.01.016. [PubMed: 21241809]

Langeslag SJE, Schmidt M, Ghassabian A, Jaddoe VW, Hofman A, van der Lugt A, Verhulst FC, Tiemeier H, White TJH, 2013 Functional connectivity between parietal and frontal brain regions and intelligence in young children: the Generation R study. Hum. Brain Mapp 10.1002/hbm.22143.

Liang Z, Liu X, Zhang N, 2015 Dynamic resting state functional connectivity in awake and anesthetized rodents. Neuroimage. 10.1016/j.neuroimage.2014.10.013.

Llera A, Wolfers T, Mulders P, Beckmann CF, 2019 Inter-individual differences in human brain structure and morphology link to variation in demographics and behavior. Elife. 10.7554/eLife.44443.

Ly M, Motzkin JC, Philippi CL, Kirk GR, Newman JP, Kiehl KA, Koenigs M, 2012 Cortical thinning in psychopathy. Am. J. Psychiatr 10.1176/appi.ajp.2012.11111627.

Ma Y, Hamilton C, Zhang N, 2017 Dynamic connectivity patterns in conscious and unconscious brain. Brain connect. 10.1089/brain.2016.0464.

Margulies DS, Ghosh SS, Goulas A, Falkiewicz M, Huntenburg JM, Langs G, Bezgin G, Eickhoff SB, Castellanos FX, Petrides M, Jefferies E, Smallwood J, 2016 Situating the default-mode network along a principal gradient of macroscale cortical organization. Proc. Natl. Acad. Sci. Unit. States Am 113, 12574–12579. 10.1073/pnas.1608282113.

Marrelec G, Krainik A, Duffau H, Pélégrini-Issac M, Leh ericy S, Doyon J, Benali H, 2006 Partial correlation for functional brain interactivity investigation in functional MRI. Neuroimage. 10.1016/j.neuroimage.2005.12.057.

Martuzzi R, Ramani R, Qiu M, Rajeevan N, Constable RT, 2010 NeuroImage Functional connectivity and alterations in baseline brain state in humans. Neuroimage 49, 823–834. 10.1016/j.neuroimage.2009.07.028. [PubMed: 19631277]

Miller KL, Alfaro-Almagro F, Bangerter NK, Thomas DL, Yacoub E, Xu J, Bartsch AJ, Jbabdi S, Sotiropoulos SN, Andersson JLR, Griffanti L, Douaud G, Okell TW, Weale P, Dragonu I, Garratt S, Hudson S, Collins R, Jenkinson M, Matthews PM, Smith SM, 2016 Multimodal population brain imaging in the UK Biobank prospective epidemiological study. Nat. Neurosci 19, 1523–1536. 10.1038/nn.4393. [PubMed: 27643430]

Müller M, Kowalewski R, Metzler S, Stettbacher A, Rössler W, Vetter S, 2013 Associations between IQ and alcohol consumption in a population of young males: a large database analysis. Soc. Psychiatr. Psychiatr. Epidemiol 10.1007/s00127-013-0666-2.

Narayan VM, Narr KL, Kumari V, Woods RP, Thompson PM, Toga AW, Sharma T, 2007 Regional cortical thinning in subjects with violent antisocial personality disorder or schizophrenia. Am. J. Psychiatr 164, 1418–1427. 10.1176/appi.ajp.2007.06101631. [PubMed: 17728428]

Narr KL, Woods RP, Thompson PM, Szeszko P, Robinson D, Dimtcheva T, Gurbani M, Toga AW, Bilder RM, 2007 Relationships between IQ and regional cortical gray matter thickness in healthy adults. Cerebr. Cortex 17, 2163–2171. 10.1093/cercor/bhl125.

Pandya Deepak, Seltzer Benjamin, Petrides Michael, C PB, 2015 Cerebral cortex: Architecture,Connections and the dual origin concept, cerebral cortex: Architecture,Connections and the dual origin concept. 10.1093/cercor/bhn205.

Pearson K, 1901 On lines and planes of closets fit to systems of points in the space. Philos. Mag. A

Reardon PK, Seidlitz J, Vandekar S, Liu S, Patel R, Park MTM, Alexander-Bloch A, Clasen LS, Blumenthal JD, Lalonde FM, Giedd JN, Gur RC, Gur RE, Lerch JP, Chakravarty MM, Satterthwaite TD, Shinohara RT, Raznahan A, 2018 Normative brain size variation and brain shape diversity in humans. Science 80 10.1126/science.aar2578.

Rosenberg MD, Finn ES, Scheinost D, Papademetris X, Shen X, Constable RT, Chun MM, 2015 A neuromarker of sustained attention from whole-brain functional connectivity. Nat. Neurosci 19, 165–171. 10.1038/nn.4179. [PubMed: 26595653]

Salimi-Khorshidi G, Douaud G, Beckmann CF, Glasser MF, Griffanti L, Smith SM, 2014 Automatic denoising of functional MRI data: combining independent component analysis and hierarchical fusion of classifiers. Neuroimage. 10.1016/j.neuroimage.2013.11.046.

Schnack HG, Van Haren NEM, Brouwer RM, Evans A, Durston S, Boomsma DI, Kahn RS, Pol HEH, 2015 Changes in Thickness and Surface Area of the Human Cortex and their Relationship with Intelligence 10, pp. 1608–1617. 10.1093/cercor/bht357.

Smilde AK, Måge I, Næs T, Hankemeier T, Lips MA, Kiers HAL, Acar E, Bro R, 2017 Common and distinct components in data fusion. J. Chemom 10.1002/cem.2900.

Smith SM, Nichols TE, Vidaurre D, Winkler AM, Behrens TEJ, Glasser MF, Ugurbil K, Barch DM, Van Essen DC, Miller KL, 2015 A positive-negative mode of population covariation links brain connectivity, demographics and behavior. Nat. Neurosci 18, 1565–1567. 10.1038/nn.4125. [PubMed: 26414616]

Song M, Zhou Y, Li J, Liu Y, Tian L, Yu C, Jiang T, 2008 Brain spontaneous functional connectivity and intelligence. Neuroimage. 10.1016/j.neuroimage.2008.02.036.

Spearman C, 1904 " general intelligence," objectively determined and measured author (s): C . Spearman Source. Am. J. Psychol 15 (2), 201–292 (4 ., 1904), pp . 201–292 Published by : University of Illinois Press Stable. http://www.jsto.15.

Thijssen S, Ringoot AP, Wildeboer A, Bakermans-Kranenburg MJ, El Marroun H, Hofman A, Jaddoe VWV, Verhulst FC, Tiemeier H, van IJzendoorn MH, White T, 2015 Brain morphology of childhood aggressive behavior: a multi-informant study in school-age children. Cognit. Affect Behav. Neurosci 15, 564–577. 10.3758/s13415-015-0344-9. [PubMed: 25801924]

Topiwala H, Terrera GM, Stirland L, Saunderson K, Russ TC, Dozier MF, Ritchie CW, 2018 Lifestyle and neurodegeneration in midlife as expressed on functional magnetic resonance imaging: a systematic review. Alzheimer's Dement. Transl. Res. Clin. Interv 10.1016/j.trci.2018.04.001.

van Dijk KRA, Sabuncu MR, Buckner RL, 2012 The influence of head motion on intrinsic functional connectivity MRI. Neuroimage. 10.1016/j.neuroimage.2011.07.044.

Van Essen DC, Smith SM, Barch DM, Behrens TEJ, Yacoub E, Ugurbil K, 2013 The Wu-minn human connectome Project: an overview. Neuroimage 80, 62–79. 10.1016/j.neuroimage.2013.05.041. [PubMed: 23684880]

V azquez-Rodríguez B, Su arez LE, Markello RD, Shafiei G, Paquola C, Hagmann P, Van Den Heuvel MP, Bernhardt BC, Spreng RN, Misic B, 2019 Gradients of structure–function tethering across neocortex. Proc. Natl. Acad. Sci. U. S. A 10.1073/pnas.1903403116.

Zhu X, Wang K, Chen L, Cao A, Chen Q, Li J, Qiu J, 2018 Together means more happiness: relationship status moderates the association between brain structure and life satisfaction. Neuroscience 384, 406–416. 10.1016/j.neuroscience.2018.05.018. [PubMed: 29792905]

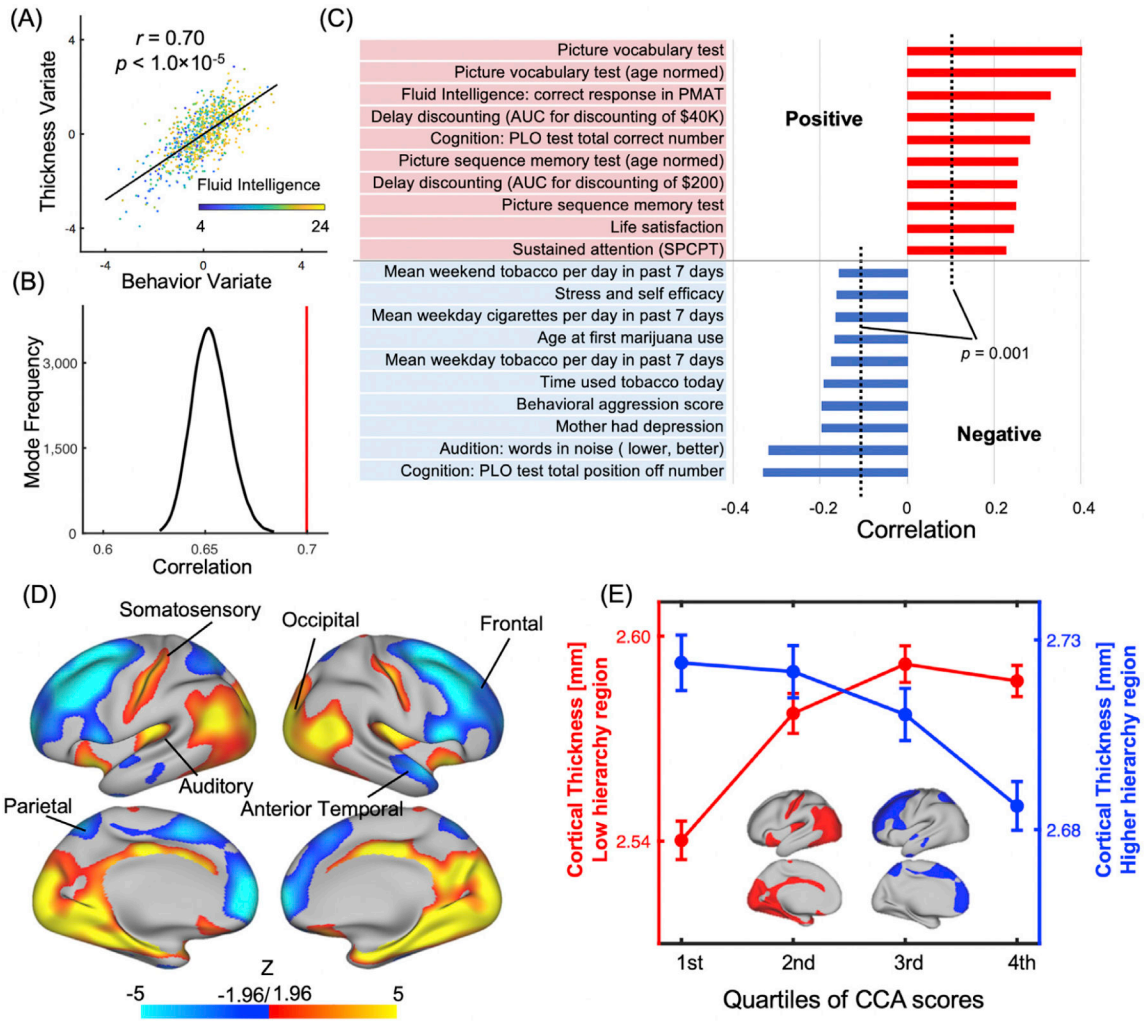

Fig. 1. The CCA mode linking the cortical thickness and behavioral/demographic measures.

(**A**) A scatter plot shows the correlation ($r = 0.70$, $p < 1.0 \times 10^{-5}$) between the two canonical variates of the identified thickness-behavior CCA mode, with one dot representing a subject. Fluid intelligence scores are color-coded the dots of the plot. (**B**) The null distribution of CCA correlations (the most significant pair) between the cortical thickness and 129 subject measures with permuting subject ID 100,000 times for the subject measures. The red line indicates the CCA correlation without permutation, i.e., the identified thickness-behavior CCA mode. (**C**) The top subject measures most strongly correlated with the identified thickness-behavior CCA mode. The positively correlated subject measures (red) generally describe positive personal traits, whereas the negatively correlated subject measures (blue) are commonly perceived as negative personal traits. (**D**) The correlations between local cortical thickness and the identified CCA mode. The original correlations are converted to Fisher's z scores. Positive correlations (red-yellow colors) are mostly seen at the lower-level sensory/motor regions, whereas negative correlations (blue-cyan colors) are more dominant at the higher-order cognitive brain regions. (**E**) The mean cortical thickness of the lower-order (red) and higher-order (blue) cortical regions in four subgroups of subjects divided by

the quartiles of the CCA score, i.e., the mean of the thickness and behavior canonical variates. Error bars represent the standard error of the mean (SEM) across subjects.

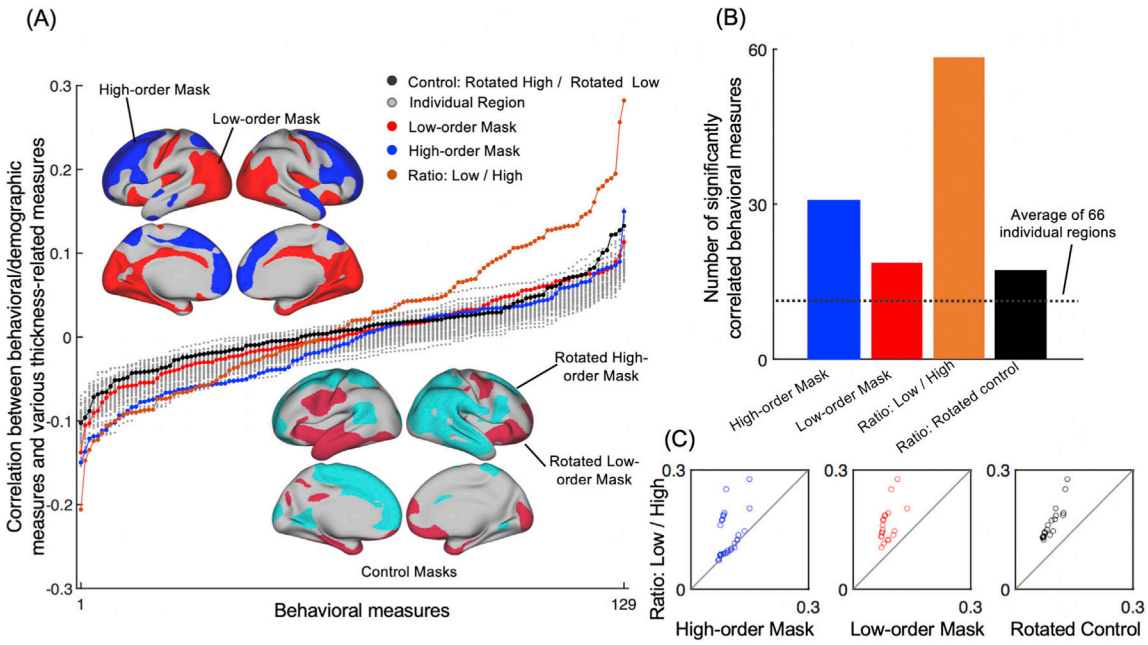

Fig. 2. Correlations between behavioral/demographic measures and various thickness measures.

(**A**) Sorted correlations between 129 behavioral/demographic measures and 70 different thickness measures, including the mean cortical thickness of 66 pre-defined brain parcels (Desikan et al., 2006) (gray lines), of the lower-(red line) and higher-order (blue line) masks, the thickness ratio between these two masks (orange line), as well as the thickness ratio between two control masks obtained by randomly rotating the lower- and higher-order masks on the brain surface (black line). (**B**) The number of significantly correlated subject measures ($p < 0.05$, uncorrected) was counted for four thickness measures. The thickness ratio between the low- and high-hierarchy regions is significantly correlated with 58 subject measures, which are much higher than the other three thickness measures. The dashed line denotes the average number of significantly correlated subject measures for the 66 individual brain parcels. (**C**) For each pair of thickness measures, a scatter plot shows their respective correlation strength (absolute correlation) with single subject measures that are significantly correlated with both (one circle per subject measure). The thickness ratio between the low- and high-hierarchy regions has a higher correlation with all the subject measures, as compared with the other three thickness measures.

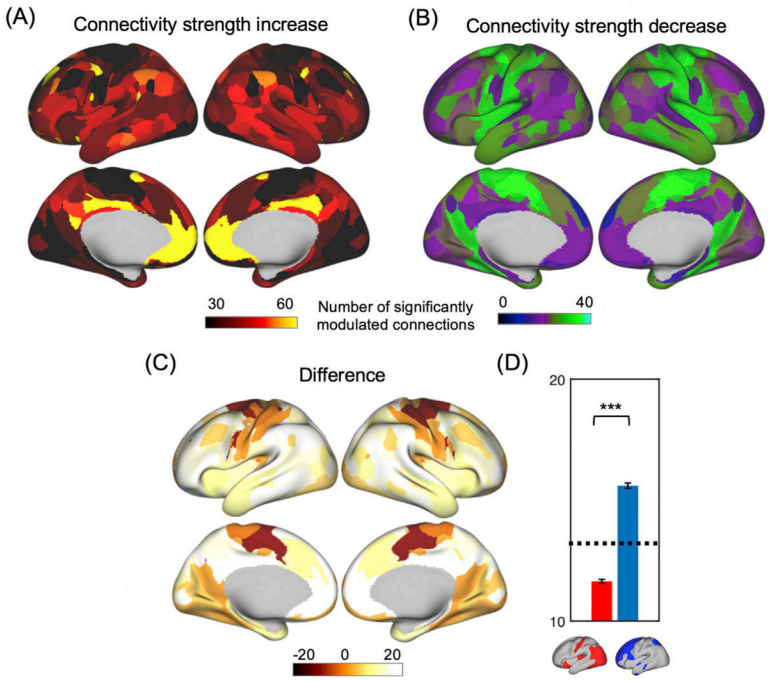

Fig. 3. Functional connectivity strength modulations along the identified connectivity-behavior CCA mode.

(**A**) Map of functional connectivity strength increase along the connectivity-behavior CCA mode towards subjects with more positive traits. The color of each brain region encodes the number of its connections (out of 199) whose strength increases significantly (i.e., upregulated) along the direction of the connectivity-behavior CCA mode. (**B**) Map of functional connectivity strength decrease along the connectivity-behavior CCA mode. The color of each brain region encodes the number of the connections whose strength decreases significantly (i.e., down-regulated) along the direction of the connectivity-behavior CCA mode. (**C**) The difference map between the two shows how much more upregulated connections than downregulated ones for each region. (**D**) A bar plot summarizes the values of the difference map (**C**) within the lower- (blue) and high-order (red) brain regions. They are not only significantly different from each other ($p = 0$), but both are also significantly different ($p = 0$) from the mean values over the whole brain (the dashed line). Error bars represent the SEM across regions.

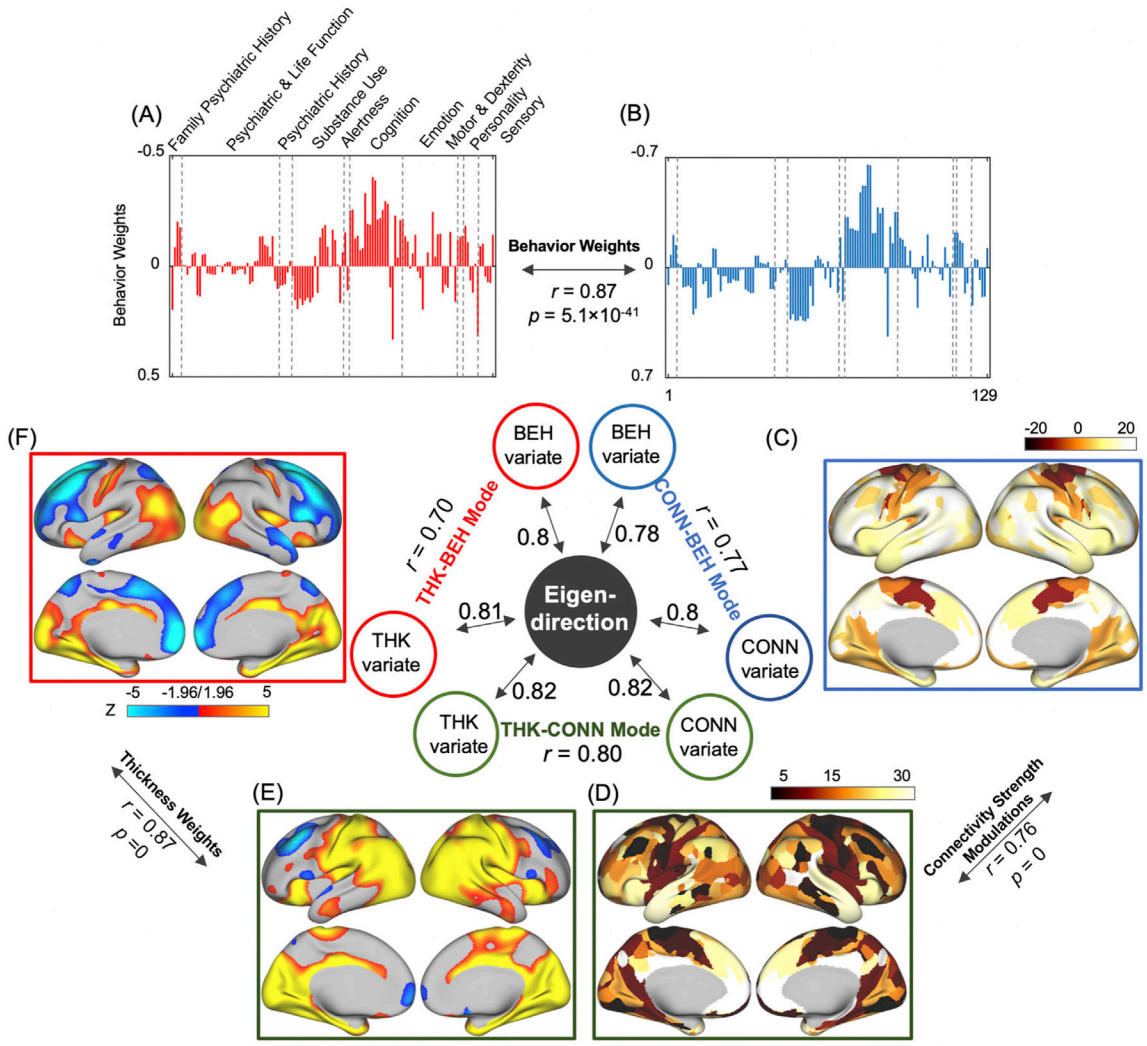

Fig. 4. The relationships between the three pairwise CCA results.

Three pairs of canonical variates from the three CCA show strong correlations with each other. The eigen-direction of the 6 canonical variates accounts for the majority of their variance (64.93%) and is strongly correlated with each one of them (correlation coefficients ranging from 0.78 to 0.82, all $p \leq 9.37 \times 10^{-170}$). The same modality of data, i.e., the behavioral/demographic measures (A–B), functional connectivity (C–D), and the cortical thickness (E–F), shows largely similar patterns of correlations with different CCA modes. All the correlations shown in this figure are statistically significant (all $p < 1.0 \times 10^{-5}$).